J. Mod. Transport. (2017) 25(2):124–131
DOI 10.1007/s40534-017-0131-0

www.springer.com/40534

A dynamic simulation of the wheel–rail impact caused by a wheel flat using a 3-D rolling contact model

Liangliang Han[1] · Lin Jing[1] · Kai Liu[1]

Received: 15 January 2017 / Revised: 25 April 2017 / Accepted: 3 May 2017 / Published online: 12 May 2017

Abstract A three-dimensional (3-D) wheel-rail rolling contact model with a wheel flat was built using commercial software Hypermesh, and the dynamic finite element simulation was conducted using LS-DYNA 3D/explicit code. Influences of the train speed, flat length and axle load on the vertical wheel-rail impact response were discussed, respectively. The results show that the maximum vertical wheel-rail impact force induced by the wheel flat is higher than that generated by the perfect wheel, and these two dynamic impact forces are much greater than the static axle load. Besides, the maximum von Mises equivalent stress and maximum equivalent plastic strain are observed on the wheel-rail contact surface, and both of them as well as the maximum wheel-rail impact force are sensitive to train speed, flat length and axle load.

Keywords High-speed train · Wheel–rail impact · Wheel flat · FE simulation

1 Introduction

The wheel flat is a common tread defect, which is usually caused by wheel–rail abrasion during the braking and rolling of wheels over long periods of time. In service, the flated wheel impact circularly against the rail, resulting in the large wheel–rail impact force and high-frequency vibration, which will bring severe damages to the wheelset, rail and track structure. The accumulation of these damages may be the potential incentive to cause the wheel/rail failure, which brings surely to the disastrous consequence and enormous economic cost. This issue has increasingly become an academic focus in the field of rail transportation. In fact, the wheel flat problem has been widely studied over the past few decades by field experiments [1–4], theoretical modeling [5–9] and finite element simulations [10–12]. Some conclusions on the influence of different out-of-round (OOR) treads on the vertical dynamic wheel–rail contact force and track response have been obtained from extensive field tests, while a number of theoretical models have been proposed for predicting the flat-induced wheel–rail response via introducing the relative displacement excitation into the Hertzian contact model [5–8] or via the non-Hertzian contact model based on the Kalker's variational method [9]. Recently, the finite element simulation has been increasingly employed to investigate the wheel–rail interaction. However, most of early developed numerical models [10–12] for the wheel–rail impact analyses are unable to well reflect the wheel–rail dynamic contact and real geometry situation of the wheel flat. In the high-speed cases, the dynamic wheel–rail interaction is governed by the inertia of the wheel and rail and is strongly dependent on geometrical, material and contact nonlinearities. Consequently, the wheel–rail rolling contact finite element models [13–15] were developed to study the wheel–rail interaction.

In this study, a three-dimensional wheel–rail rolling contact model with a flat was built using commercial software Hypermesh, and the corresponding dynamic simulation was conducted using LS-DYNA 3D explicit algorithm, while both the inertia effect of the wheel–rail system and the dynamic nonlinearity were considered. Influences of the train speed, flat length and axle load, on

✉ Lin Jing
jinglin@home.swjtu.edu.cn; jinglin_426@163.com

[1] State Key Laboratory of Traction Power, Southwest Jiaotong University, 111 North Section 1, Second Ring Road, Chengdu 610031, Sichuan Province, China

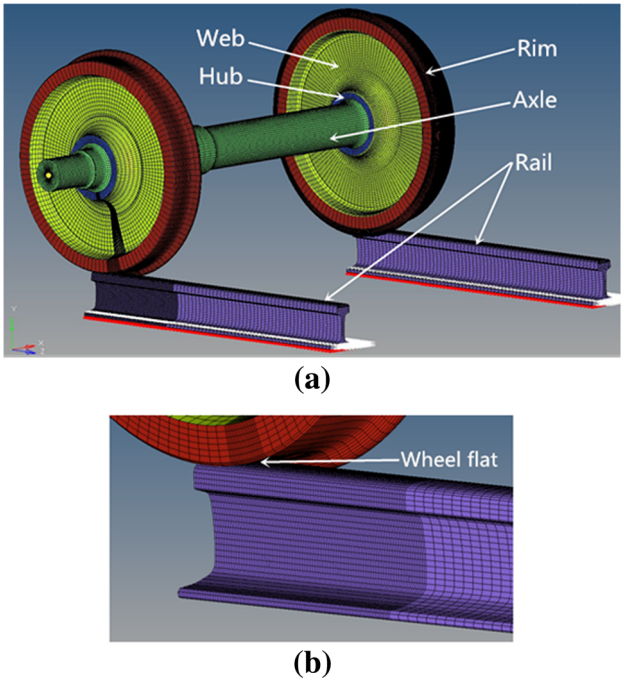

Fig. 1 FE model of the wheel–rail system with a 60-mm flat length. **a** Overall wheel–rail rolling contact model. **b** Enlarged view of the flat zone

the vertical wheel–rail impact force response were discussed over a wide range.

2 Finite element model

The whole finite element model for wheel–rail rolling contact was built using commercial software Hypermesh, which includes two wheels (the one with a fresh flat), one axle and two rails. The wheel has a S1002CN tread and the radius of 430 mm, while the rail is the 60 kg/m steel rail with a base slope of 1:40. A typical three-dimensional wheel–rail rolling contact model with single 60-mm flat is shown in Fig. 1. Due to the short duration (around several milliseconds) of the wheel–rail impact process, it has no time to transfer impact load to the infrastructure below the rail, and thus, the rail bears the impact load directly. The infrastructure below the rail is omitted in the present study to save the computational cost. The wheel–rail finite element model was fine meshed by 8-node solid element with the size of 4 mm × 4 mm in the flat contact area, while the rest were medially meshed. The whole FE model consists of 515,108 nodes and 477,290 elements.

The wheel and rail were described by the material model *MAT_PLASTIC_KINEMATIC, while the axle was represented by the model *MAT_RIGID. The material parameters used in the simulations are listed in Table 1. All the nodal DOFs of the rail bottom were constrained to simulate the clamped boundary conditions, and an axial translational constraint was set to two ends of the rigid axle. The gravitational acceleration was endowed to the whole wheel–rail system. Two constant forces were applied to the axle to represent the static vehicle weight, which are the equivalent loads converted from the axle load according to the criterion of EN13104 [16]. For 17 t axle load, the value of the larger force is 110.41 kN and the smaller force is 77.56 kN. Automatic, surface-to-surface contact options were generally used for the whole wheel–rail system.

3 Simulation results and discussion

The validation of the proposed wheel–rail rolling contact finite element model with a wheel flat has been demonstrated in our previous study [17], and the details are omitted here to avoid the repetition.

3.1 Typical vertical wheel–rail impact response

Figure 2 shows a typical vertical wheel–rail impact force versus time curve induced by a wheel flat for the 60-mm flat, 200 km/h train speed of and 17 t axle load case. It is found that, during the impact process of the flated wheel against the rail, the first peak vertical wheel–rail impact force occurs at 2.5 ms, and its amplitude is around 325 kN, which is approximately 3.46 times larger than the average static axle load of 93.99 kN. Beyond 2.5 ms, the impact force is reduced gradually to zero, since the vertical dynamic contact force is larger significantly than the sum of the axle load and gravity, resulting in a transient

Table 1 Material parameters of components of the wheel–rail system

Components	Elastic modulus (GPa)	Density (kg/m^3)	Poisson ratio	Yield stress (MPa)	Tangent modulus (GPa)
Rim	213	7800	0.3	561	21
Web	216	7800	0.3	395	21
Hub	213	7800	0.3	417	21
Axle	206	7800	0.3	–	–
Rail	193	7800	0.3	525	19

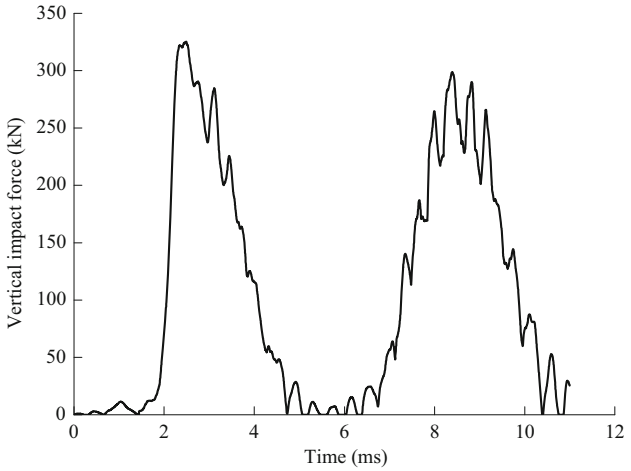

Fig. 2 Time history curve of typical vertical wheel–rail impact force under the train speed of 200 km/h, flat length of 60 mm and axle load of 17 t

separation between the wheel and rail. Subsequently, the wheel falls back due to its gravity and impact against the rail again. However, the second peak of vertical impact force is caused by the intact wheel part impacting against the rail as the wheel has rolled out of the flat spot. Obviously, the second peak force appears at 8.3 ms and the magnitude is around 300 kN, which is around 0.923 times over that with a flat.

The typical von Mises equivalent stress and maximum shear stress responses of the element with the global maximum von Mises equivalent stress are presented in Fig. 3. It is shown that the von Mises equivalent stress and maximum shear stress are in a small fluctuations before 2.1 ms and then experience a sharp increase to the corresponding maximum values of 672 and 382 MPa at approximately 3.0 ms (the wheel impact against the rail),

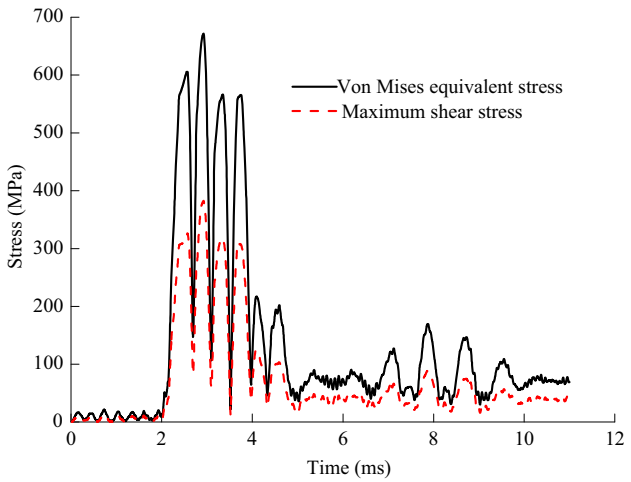

Fig. 3 Von Mises equivalent stress and maximum shear stress history curves

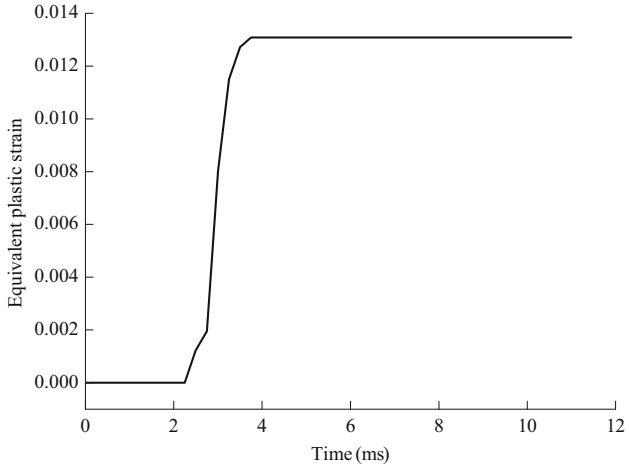

Fig. 4 Equivalent plastic strain history curve

followed with great fluctuations. After 3.0 ms, the von Mises equivalent stress and maximum shear stress decrease rapidly and stabilize at the lower stress levels, respectively. It should be noted that the maximum von Mises equivalent stress (672 MPa) of the wheel rim is much larger than the yield stress of the wheel rim (561 MPa), which may cause the local plastic deformation of the wheel rim. Figure 4 provides the equivalent plastic strain versus time curve, where the maximum equivalent plastic strain of 0.013 is obtained.

Figure 5a, b shows the typical von Mises equivalent stress contours and equivalent plastic strain contours of the wheel/rail component along the rolling direction, respectively, where the train speed is set to be 200 km/h, the flat length is 60 mm and axle load is 17 t. It is obvious that both the maximum von Mises equivalent stress (667.6 MPa) and maximum equivalent plastic strain (0.013) occur on the wheel–rail contact surface.

3.2 Influence of train speed

To investigate the influence of train speed on the vertical wheel–rail impact response, six train speeds (i.e., 100, 150, 200, 250, 300 and 350 km/h) were selected. Figure 6a shows a typical set of the vertical wheel–rail impact force versus time curves induced by a 60-mm flat for a given axle load of 17 t. It is observed that the history curves of vertical force response at six different train speeds are similar, and the maximum vertical impact force has a non-monotonic change with train speed, i.e., it increases with the train speed up to the peak value of 325 kN for the speed less than or equal to 150 km/h and then decreases slowly with the speed up to 350 km/h. The maximum vertical wheel–rail impact forces induced by a wheel flat are plotted in Fig. 6b, which is a function of the train speed. The non-monotonic relationships between the maximum vertical

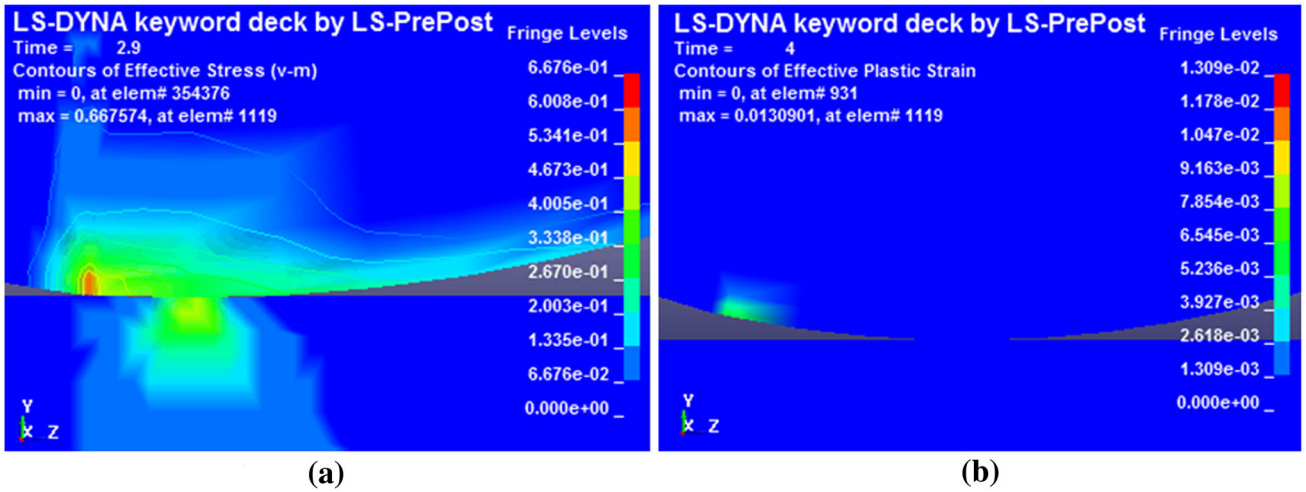

Fig. 5 Von Mises equivalent stress and equivalent plastic strain contours. **a** Von Mises equivalent stress contour. **b** Equivalent plastic strain contour

impact force and train speed for all flat lengths are clearly presented, and the peak values of maximum vertical impact forces occur at train speed of 150 km/h for the flat length less than or equal to 60 mm, while the peak value induced by the wheel flat occurs at the train speed of 200 km/h for the 80-mm flat spot. This non-monotonic relationship between the peak vertical force and train speed may be related with the loss of contact under different speeds, and the reason that the peak contact force for the 80-mm flat occurs at a higher speed than those for other flats is related to the contact position of the flat with the rail. The closer the impact point and the flat tip are to each other. For the flat lengths of 20, 40 and 60 mm, the impact point locates next the flat tip at the train speed of 150 m/s, thus generating the peak value at this speed; however, for the flat length of 80 mm, it takes the more time for the impact point to close the flat tip; thus, a higher speed of 200 km/h is required.

Figures 7 and 8 show the global maximum von Mises equivalent stress and maximum equivalent plastic strain of the wheel as a function of train speed, respectively. It is shown from Fig. 7 that the maximum von Mises equivalent stress increases firstly with train speed and reaches a peak value and then decreases with the speed. When the flat length is less than or equal to 60 mm, the maximum von Mises equivalent stress peaks at the speed of 200 km/h; when the flat length is equal to 80 mm, it peaks at the speed of 150 km/h. It is also noted that the higher stress value induced by a wheel flat will cause the local plastic deformation of the wheel. It can be seen from Fig. 8 that the maximum equivalent plastic strain changes in a way similar to the maximum

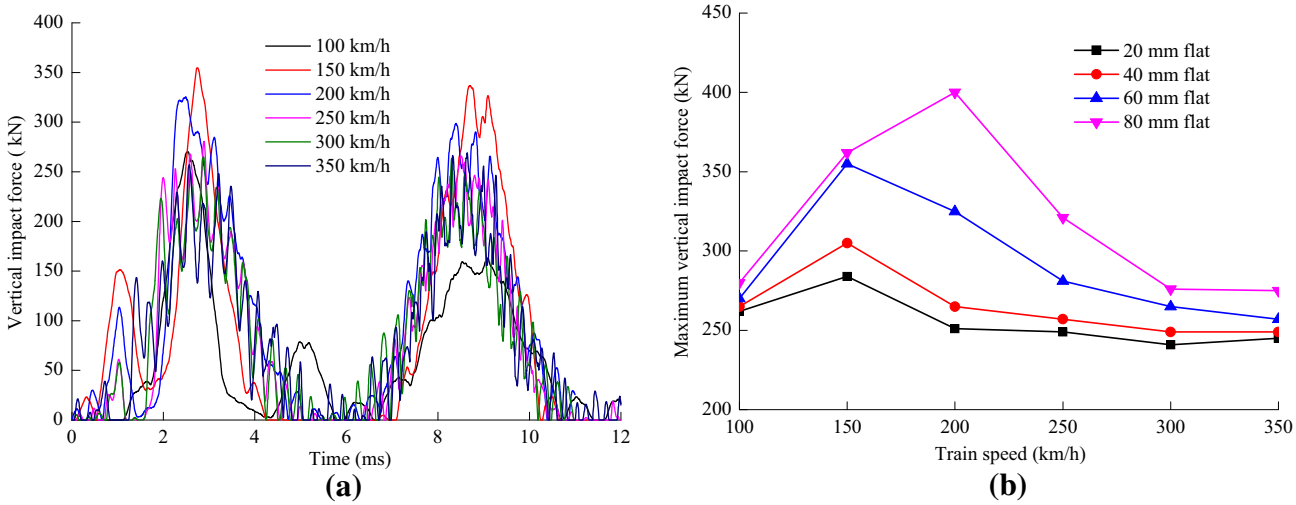

Fig. 6 Influence of train speed on the vertical wheel–rail impact response. **a** Vertical impact force–time curves. **b** Maximum vertical impact force as a function of train speed

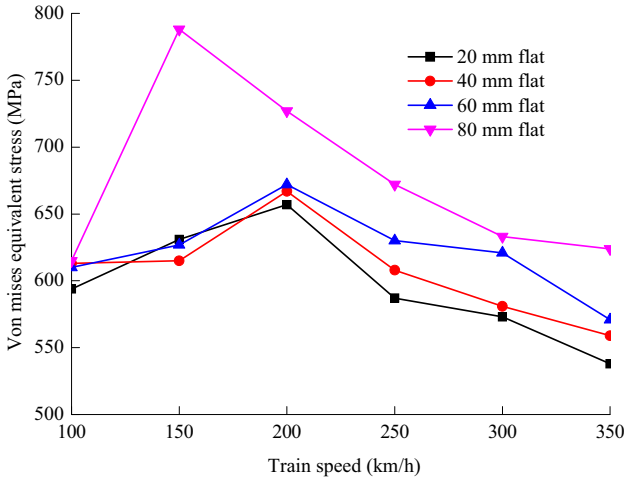

Fig. 7 Maximum von Mises equivalent stress as a function of train speed

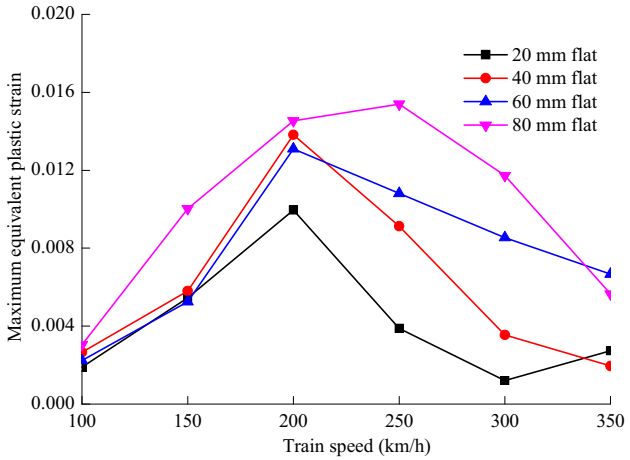

Fig. 8 Maximum equivalent plastic strain as a function of train speed

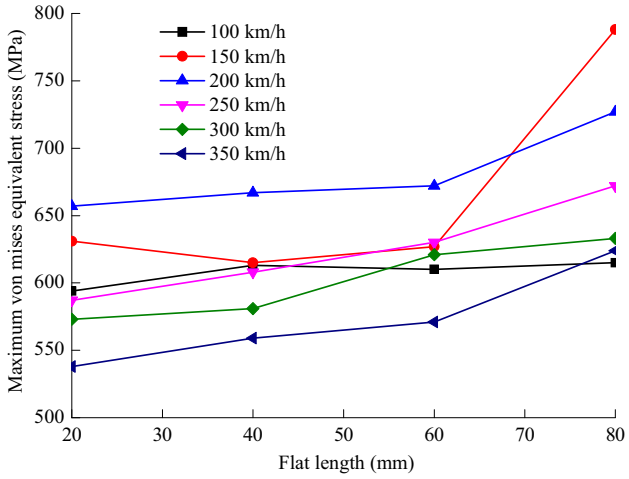

Fig. 10 Maximum von Mises equivalent stress versus a function of flat length

von Mises equivalent stress. The difference is that the peak value of maximum equivalent plastic strain occurs at the speed of 250 km/h for the 80-mm flat. The large plastic deformation may gradually cause the long local defect, eventually leading to the wheel polygonal wear.

3.3 Influence of flat length

Four different flat lengths (i.e., 20, 40, 60 and 80 mm) were selected to study the influence of flat length on the vertical wheel–rail impact response, where the axle load was fixed at 17 t. Typical vertical wheel–rail impact force history curves induced by different flat lengths at the train speed of 200 km/h are plotted in Fig. 9a. It is obvious that the maximum vertical impact force induced by wheel flat increases with the flat

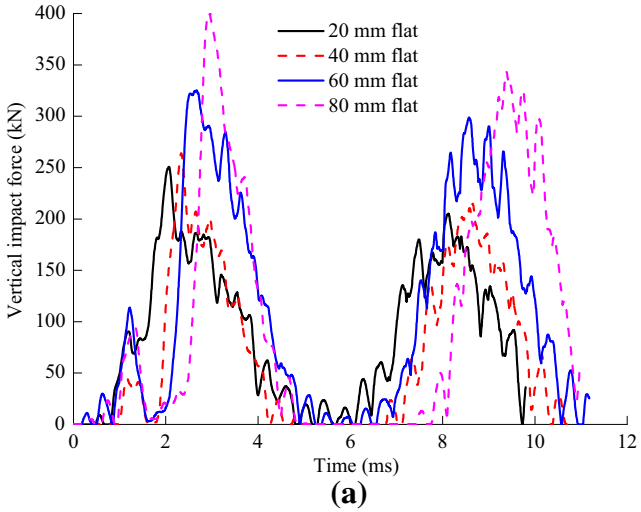

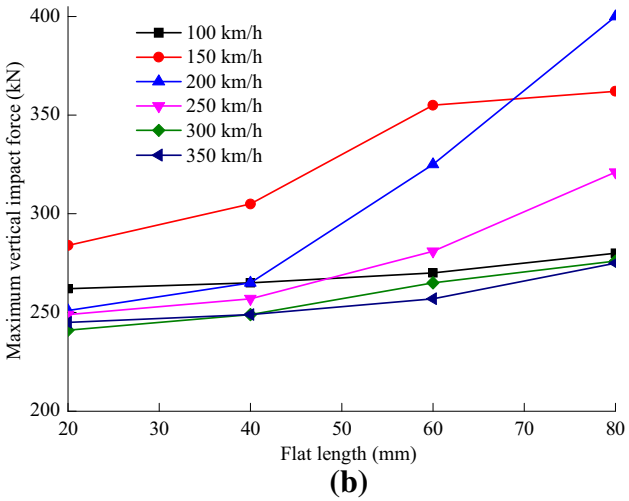

Fig. 9 Influence of flat length on the vertical wheel–rail impact response. **a** Typical vertical impact force versus time curves. **b** Maximum vertical impact force

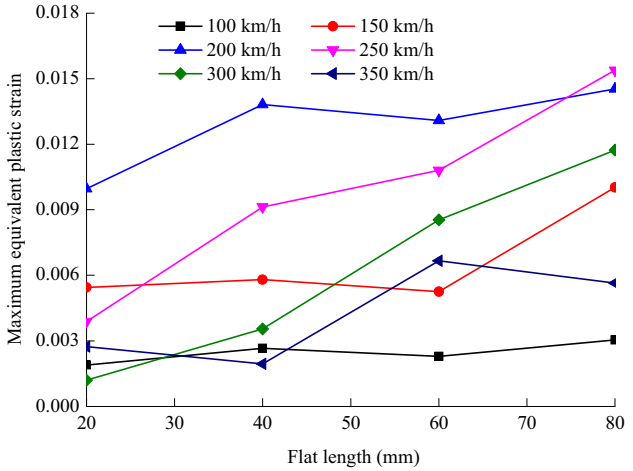

Fig. 11 Maximum equivalent plastic strain versus flat length

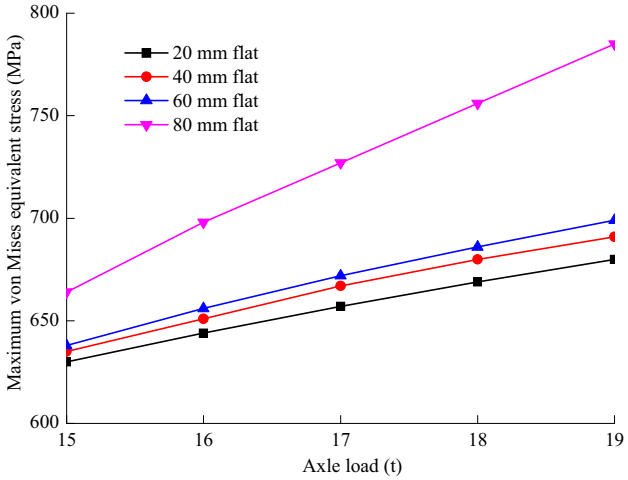

Fig. 13 Maximum von Mises equivalent stress versus axle load

length, and the peak value of the maximum vertical impact force is 400 kN for the flat length of 80 mm. It should be noted that the second peak impact forces generated by the intact wheel dropping against the rail also increase with the flat length, this is because the drop distance and time during wheel flat impacting the rail are determined by the flat length, and the longer wheel flat length will cause the larger drop distance and the later impact occurring [13], resulting in the larger impact kinetic energy. This explanation is also validated the simulated second wheel–rail impact time, that is, the longer the flat length is, and the later the second impact occurs. Figure 9b illustrates the maximum vertical wheel–rail impact forces at different train speeds as a function of the flat length. The maximum vertical impact force nonlinearly increases with the flat length, and the influence of flat length on the maximum vertical impact force seems to be significant within the speed range from 150 to 250 km/h.

Figures 10 and 11 show the influences of the flat length on the maximum von Mises equivalent stress and maximum equivalent plastic strain of the wheel, respectively. It is shown from Fig. 10 that the maximum von Mises equivalent stress under different train speeds increase with flat length. The variation of the maximum von Mises equivalent stress is slight when the flat length is less than or equal to 60 mm, while this increase is relatively larger when the flat length is greater than 60 mm and train speed exceeds 100 km/h. Besides, it can be also found from Fig. 11 that the maximum equivalent plastic strain is relatively larger at the speed of 200 km/h for the flat length less than 80 mm than those under other speed conditions.

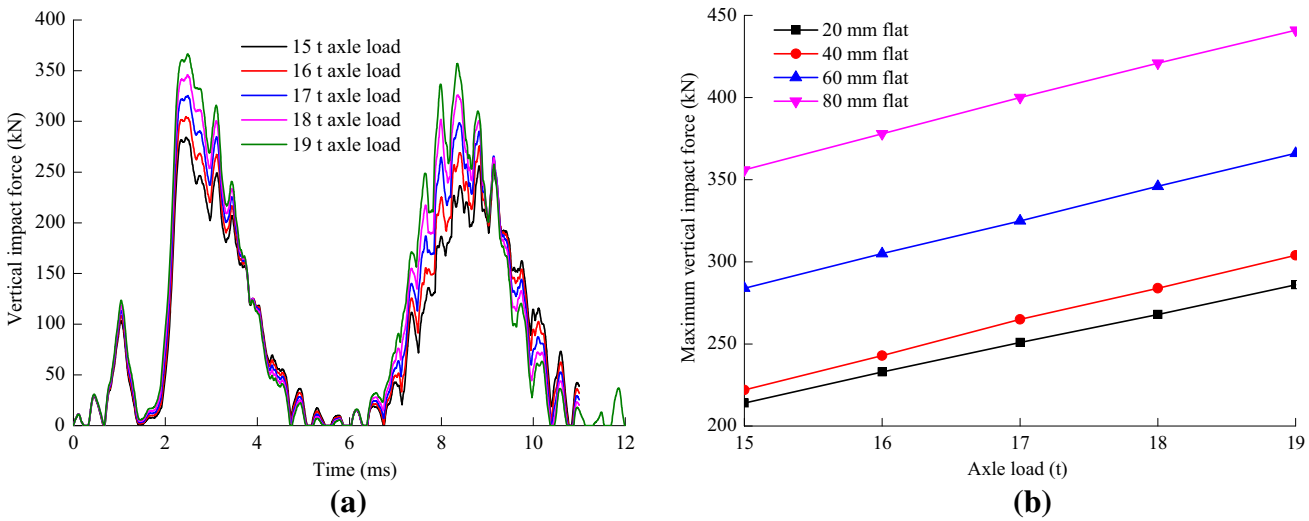

Fig. 12 Influence of axle load on the vertical wheel–rail impact response. **a** Typical vertical impact force versus time curves. **b** Maximum vertical impact force

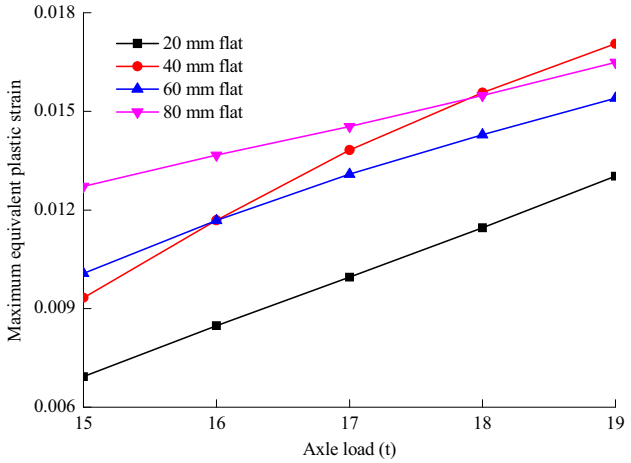

Fig. 14 Maximum equivalent plastic strain versus axle load

3.4 Influence of axle load

For a given flat length of 60 mm and train speed of 200 km/h, five different axle loads (i.e., 15, 16, 17, 18 and 19 t) were selected to study the influence of axle load on the wheel–rail impact response. Typical vertical wheel–rail impact force versus time curves with a 60-mm flat under different axle loads are shown in Fig. 12a. The similar trend of the vertical wheel–rail impact force changing with time is observed for five different axle load cases, and the vertical impact force is increased with the axle load. The maximum vertical impact forces versus axle load with different flat lengths are plotted in Fig. 12b. It is shown that a linear increase relationship between the maximum vertical impact force and axle load is found for each flat length case.

Figures 13 and 14 show the maximum von Mises equivalent stress and maximum equivalent plastic strain versus axle load, respectively. As seen in Fig. 13, the maximum von Mises equivalent stress increases approximately linearly with the axle load for each flat length. Similarly, the large von Mises equivalent stress may cause the local plastic deformation of the wheel rim. Thus, the maximum equivalent plastic strain is also presented in Fig. 14, and an approximately linear relationship between the maximum equivalent plastic strain and axle load is observed for a given flat length.

4 Conclusions

A three-dimensional wheel–rail rolling contact model with a wheel flat was built for analyzing the wheel–rail impact response induced by the wheel flat. Influences of the train speed, flat length and axle load on the vertical wheel–rail impact response were discussed, respectively. Some main conclusions are drawn as follows: (1) the maximum vertical wheel–rail impact forces are greater significantly than the corresponding static axle loads due to the presence of a wheel flat; (2) the maximum von Mises equivalent stress and maximum equivalent plastic strain occur on the wheel–rail contact surface, and they are sensitive to the train speed, flat length and axle load; (3) the wheel–rail impact force caused by a flat has non-monotonic change with the train speed, and the corresponding peak value occurs within the range from 150 to 200 km/h; (4) the vertical impact force increases with the flat length, and the approximately linear relationship between the maximum values of wheel–rail impact responses (including the force, von Mises equivalent stress and equivalent plastic strain) and axle load is found for each flat length.

Acknowledgements This study is supported by the National Natural Science Foundation of China (Grant No. 51475392), the Fundamental Research Funds for the Central Universities (Grant No. 2682015RC09) and the Research Fund of State Key Laboratory of Traction Power (Grant No. 2015TPL_T02). The authors greatly appreciate the financial support.

References

1. Newton SG, Clark RA (1979) An investigation into the dynamic effects on the track of wheel flats on railway vehicles. J Mech Eng Sci 21:287–297
2. Fermér M, Nielsen JCO (1995) Vertical interaction between train and track with soft and stiff rail pads—full-scale experiments and theory. Proc Inst Mech Eng F J Rail Rapid Transit 209:39–47
3. Jergéus J, Odenmarck C, Lundén R, Sotkovszki P, Karlsson B, Gullers P (1999) Full-scale railway wheel flat experiments. Proc Inst Mech Eng F J Rail Rapid Transit 213:1–13
4. Johansson A, Nielsen JCO (2003) Out-of-round railway wheels–wheel rail contact forces and track response derived from field tests and numerical simulations. Proc Inst Mech Eng F J Rail Rapid Transit 217:135–146
5. Nielsen JCO, Igeland A (1995) Vertical dynamic interaction between train and track influence of wheel and track imperfections. J Sound Vib 187:825–839
6. Dukkipati RV, Dong R (1999) Impact loads due to wheel flats and shells. Veh Syst Dyn 31:1–22
7. Wu TX, Thompson DJ (2002) A hybrid model for the noise generation due to railway wheel flats. J Sound Vib 251:115–139
8. Baeza L, Roda A, Carballeira J, Giner E (2006) Railway train-track dynamics for wheelflats with improved contact models. Nonlinear Dyn 45:385–397
9. Pieringer A, Kropp W, Nielsen JCO (2014) The influence of contact modelling on simulated wheel/rail interaction due to wheel flats. Wear 314:273–281

10. Thambiratnam DP, Zhuge Y (2008) Finite element analysis of track structures. Comput Aided Civ Infrastruct Eng 8: 467–476
11. Gaul L, Fischer M, Nackenhorst U (2002) FE/BE analysis of structural dynamics and sound radiation from rolling wheels. Comput Model Eng Sci 3:815–823
12. Chang C, Wang C, Chen B, Li L (2010) A study of a numerical analysis method for the wheel–rail wear of a heavy haul train. Proc Inst Mech Eng F J Rail Rapid Transit 224:473–482
13. Bian J, Gu YT, Murray MH (2013) A dynamic wheel–rail impact analysis of railway track under wheel flat by finite element analysis. Veh Syst Dyn 51:784–797
14. Zhao X, Li Z (2011) The solution of frictional wheel–rail rolling contact with a 3D transient finite element model: validation and error analysis. Wear 271:444–452
15. Zhao X, Wen ZF, Zhu MH (2014) A study on high-speed rolling contact between a wheel and a contaminated rail. Veh Syst Dyn 52:1270–1287
16. BS EN 13104-2009. Railway applications—wheelsets and bogies–powered axles–design method
17. Han LL, Jing L, Zhao LM (2017) Finite element analysis of the wheel–rail impact behavior induced by a wheel flat for high-speed trains: the influence of strain rate. Proc Inst Mech Eng F J Rail Rapid Transit. doi:10.1177/0954409717704790